Available online at www.sciencedirect.com
SCIENCE DIRECT
Journal of Solid State Chemistry 179 (2006) 1490–1496
JOURNAL OF SOLID STATE CHEMISTRY
www.elsevier.com/locate/jssc

A Raman spectroscopic study of the phase transition of $BaZr(PO_4)_2$: Evidence for a trigonal structure of the high-temperature polymorph

Thorsten Geisler[a,*], Karin Popa[b,c], Rudy J.M. Konings[b], Aurelian F. Popa[d]

[a]*Institut für Mineralogie, Westfälische Wilhelms-Universität, Corrensstr. 24, 48149 Münster, Germany*
[b]*European Commission, Joint Research Centre, Institute for Transuranium Elements, P.O. Box 2340, 76125 Karlsruhe, Germany*
[c]*"Al.I. Cuza" University, Department of Inorganic and Analytical Chemistry, 11-Carol I Blvd., 700506 Iasi, Romania*
[d]*Faculté des Sciences-Université de Nantes, Institut des Matériaux Jean Rouxel-Laboratoire de Chimie des Solides 2, rue de la Houssinière, B.P. 32229, 44322 Nantes Cedex 3, France*

Received 23 December 2005; received in revised form 30 January 2006; accepted 31 January 2006
Available online 9 March 2006

Abstract

We have studied the structural evolution of monoclinic $BaZr(PO_4)_2$ during heating up to 835 K by Raman spectroscopy. In agreement with previous studies we found a first-order phase transition at about 730 K during heating while upon cooling the reverse transition occurs at 705 K. However, some disagreement about the crystal structure of the high-temperature polymorph occurs in the literature. While the space group has not yet been determined, the X-ray diffraction pattern of the high-temperature phase has been indexed on either an orthorhombic or a hexagonal unit cell. We found that the number of Raman active internal PO_4 vibrational modes decrease from nine to six during the transition. A group theoretical survey through all orthorhombic, trigonal, and hexagonal factor groups revealed that the observed number of vibrations would only be consistent with the Ba and Zr atoms located at a $D_{3d}(\bar{3}m)$ site, the P and two O atoms at a $C_{3v}(3m)$, and six O atoms at a $C_s(m)$ site in the D_{3d} factor group. Based on our Raman data, the space group of the high-temperature polymorph is thus either $D^1_{3d}(P\bar{3}1m)$, $D^3_{3d}(P\bar{3}m1)$, or $D^5_{3d}(R\bar{3}m)$.

Keywords: Barium zirconium phosphate; $BaZr(PO_4)_2$; Raman spectroscopy; Phase transition

1. Introduction

Rare-earth orthophosphates such as, e.g., monazite, $CePO_4$, and brabantite, $CaTh(PO_4)_2$, are potential candidates for the immobilization of weapons-grade Pu or other highly radioactive waste produced within the nuclear fuel cycle because they show an extremely high aqueous durability and good resistance to self-irradiation damage [1,2]. Due to these properties, we have started a detailed study of various synthetic endmembers and their solid solutions. As part of this, we studied the orthophosphate compounds $AZr(PO_4)_2$ with $A = Ca$, Sr and Ba, which have a different crystal structure at room temperature [3–5]. Whereas $CaZr(PO_4)_2$ is tetragonal [3], $SrZr(PO_4)_2$ has a triclinic [4] and $BaZr(PO_4)_2$ a monoclinic ($C^3_{2h} \equiv C2/m$) yavapaiite structure [5]. During heating, $SrZr(PO_4)_2$ undergoes a triclinic to monoclinic transition at 405 K and then to hexagonal (trigonal) at 1196 K [4]. The monoclinic structure is believed to be isostructural with yavapaiite ($KFe(SO_4)_2$) and thus with the room temperature structure of $BaZr(PO_4)_2$. It has been shown that $BaZr(PO_4)_2$ also undergoes a phase transition at 730 K [5]. However, there exists some disagreement in the literature concerning the crystal structure of the high-temperature polymorph. Whereas Fukuda et al. [5] have indexed the X-ray diffraction pattern of the high-temperature phase on an orthorhombic unit cell, Popa et al. [6] assumed a hexagonal cell by analogy with the high-temperature polymorph of $SrZr(PO_4)_2$. We note here that Fukuda and coworkers mentioned that the unit cell was nearly orthohexagonal, i.e. $\sqrt{3}b \approx a$. In such a case, there are closely overlapping

*Corresponding author. Fax: +49 251 83 3 83 97.
E-mail address: tgeisler@nwz.uni-muenster.de (T. Geisler).

0022-4596/$ - see front matter © 2006 Elsevier Inc. All rights reserved.
doi:10.1016/j.jssc.2006.01.065

diffraction signals from $2h0l$ and hhl lattice planes in a powder diffraction pattern as mentioned by Fukuda and coworkers [5].

Here we report the results of a temperature-dependent Raman spectroscopic study, which was aimed (1) to investigate hard mode behavior across the phase transition of $BaZr(PO_4)_2$ and (2) to obtain further structural information about the high-temperature polymorph. Although vibrational spectroscopic methods provide a very valuable tool for obtaining information about the nature of bonding in crystalline solids, they cannot be considered as a method of structure determination. However, vibrational spectrocopy can be used to check a given crystal structure obtained by means of X-ray diffraction data. We show in the following that it is possible to determine the crystal class and the most likely space groups of the high-temperature polymorph by comparing the observed number of Raman bands with those theoretically predicted for various structural possibilities in the orthorhombic and hexagonal (trigonal) space groups.

2. Experimental details

2.1. Synthesis

$BaZr(PO_4)_2$ was synthesized by grinding and reacting equimolar quantities of $BaCO_3$ and ZrO_2 and 25% excess of $(NH_4)_2HPO_4$ in an alumina crucible after pressing the powder into a pellet. To obtain the pure compound, different synthesis attempts were made in air at temperatures between 1373 and 1473 K for 5–100 h. The optimum synthesis conditions were found to be 1473 K and 100 h reaction time. The purity of the sample was checked by powder X-ray diffraction analysis using Philips X'Pert automated powder diffractometer. The diffraction pattern (not shown here) is identical to that reported in [5]. We further note that the room-temperature Raman spectrum of barium zirconium phosphate in the frequency range between 160 and 1300 cm^{-1} (Fig. 1a) shows the same number of bands as previously reported [7], which further confirms the purity of the sample.

2.2. Raman spectroscopy

Raman measurements were conducted with a high-resolution Jobin Yvon HR800 Raman system using a Nd-YAG (532 nm) laser with ~10 mW power at the surface of the ceramic pellet in the frequency range between 160 and 1300 cm^{-1}. The scattered Raman light was collected in 180° backscattering geometry and dispersed by a grating of 1800 grooves/mm after having passed a 100 μm entrance slit, resulting in a spectral resolution of ~1.2 cm^{-1}. A ×10 objective with a numerical aperture of 0.4 was used for all measurements. The backscattered Raman signal was collected four times for 15 s. The pellet was heated in a Linkam heating stage for temperature-dependent measurements. The heating and cooling rates between the individual temperature steps were 10 K/min and the sample was equilibrated for 5 min at the desired temperature. The accuracy of the temperature was better than ±5 K.

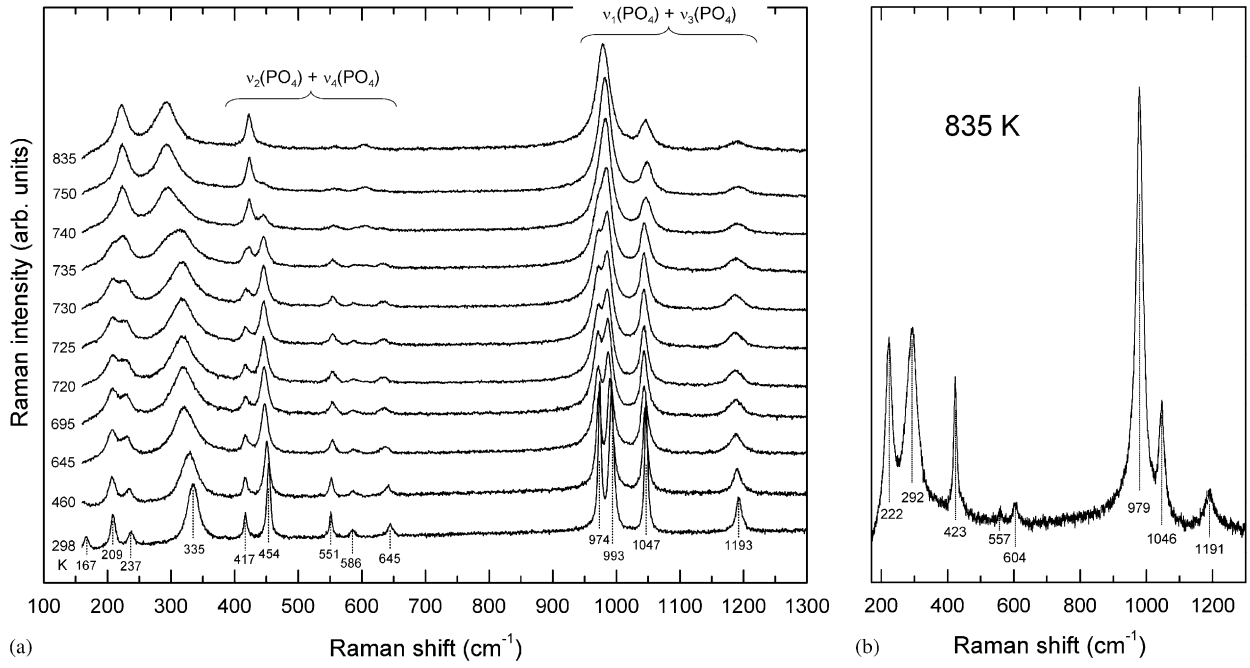

Fig. 1. (a) Stacked Raman spectra of $BaZr(PO_4)_2$ recorded at different temperatures (given on the left-hand side of each spectrum). (b) Raman spectrum from the high-temperature polymorph recorded at 835 K.

3. Crystal structure and vibrational analysis of the low-temperature polymorph

At room temperature $BaZr(PO_4)_2$ crystallizes in the monoclinic yavapaiite structure with the space group $C^3_{2h}(C2/m)$ and two molecules in the unit cell [5]. The unit cell parameters are $a = 0.85629(3)$ nm, $b = 0.53082(2)$ nm, $c = 0.789566(2)$ nm, and $\beta = 93.086(1)^\circ$. The structure consists of BaO_{10}, ZrO_6, and PO_4 polyhedra. The PO_4 tetrahedra and the BaO_{10} polyhedra share edges and form two-dimensional sheets parallel to (001). These sheets are stacked along the c direction and linked by the oxygens O(1) and O(3) to the ZrO_6 octahedra. The barium and zirconium atoms are both located at $C_{2h}(2/m)$, the phosphorus atom as well as two equivalent oxygen atoms O(1) and O(2) on a mirror plane, and the other two oxygen atoms on general positions x, y, z (C_1).

Room temperature Raman and infrared (IR) measurements and the symmetry assignment of the bands have previously been published by Paques-Ledent [7]. Group theoretical analysis based on the above-given site symmetries predicts 15 Raman and 18 IR active normal modes, which can be split into the following irreducible representation for the translational modes of the cations and of the anions, respectively [7]:

$$\Gamma_{Ba} = \Gamma_{Zr} = A_u + 2B_u,$$
$$\Gamma_{P} = 2A_g + B_g + A_u + 2B_u,$$
$$\Gamma_{O1} = \Gamma_{O2} = 2A_g + B_g + A_u + 2B_u,$$
$$\Gamma_{O3} = 3A_g + 3B_g + 3A_u + 3B_u.$$

These representations include one A_u and two B_u modes corresponding to acoustic vibrations. We note that translational movements of zirconium and barium are only IR active (symmetry species with index u).

The previous Raman spectroscopic work has detected 14 of the 15 expected bands at room temperature, which can be well separated into nine internal PO_4 modes and five external rotational and translational PO_4 modes (Fig. 1). The nine internal stretching (ν_1 and ν_3) and bending (ν_2 and ν_4) modes of the PO_4 tetrahedra were found to have frequencies between 950 and 1200 cm^{-1} and 415 and 650 cm^{-1}, respectively (Fig. 1a). The translational and rotational or better-hindered rotational (librational) bands occur at wavenumbers below 340 cm^{-1}. Based on the fact that only unpolarized Raman measurements have been carried out on polycrystalline $BaZr(PO_4)_2$ so far, a full symmetry assignment was not yet possible. However, Paques-Ledent [7] assigned the bands at 335 and 1047 cm^{-1} to a librational $R(PO_4)$ mode with A_g symmetry and an antisymmetric $\nu_3(PO_4)$ stretching vibration with B_g symmetry, respectively.

4. Results

Fig. 1a shows Raman spectra of $BaZr(PO_4)_2$ in the frequency range between 160 and 1300 cm^{-1} recorded at various temperatures. Within this frequency range 13 bands can clearly be detected in the room temperature spectrum. The spectrum resembles those previously recorded for different phosphates and arsenates with a yavapaiite structure [7]. However, due to experimental limitations, we were unable to record the Raman spectrum below 160 cm^{-1}, where Paques-Ledent [7] detected a further band near 100 cm^{-1}.

A spectrum of the high-temperature polymorph is shown in Fig. 1b. It is evident that the number of bands in the frequency range between 160 and 1300 cm^{-1} decreases from 13 to eight, whereas the number of the internal modes of the PO_4 tetrahedra decreases from nine to six, indicating that some modes degenerate.

On heating, the band intensities decrease while the bandwidths increase (Fig. 1a). The evolution of all observed peak frequencies and the intensity of the $\nu_3(PO_4)$ band near 1193 cm^{-1}, the internal PO_4 bending mode near 454 cm^{-1}, and the librational (A_g) mode 335 cm^{-1} on heating and cooling is shown in Figs. 2 and 3, respectively. These figures clearly show a hysteresis-like temperature behavior typical for first-order phase transitions. On heating, several Raman bands gradually disappear. The two bands at 993 and 974 cm^{-1} in the low-temperature polymorph merge into a single band at the transition temperature (Fig. 2). The same can be observed for the neighboring bands at 237 and 209 cm^{-1}.

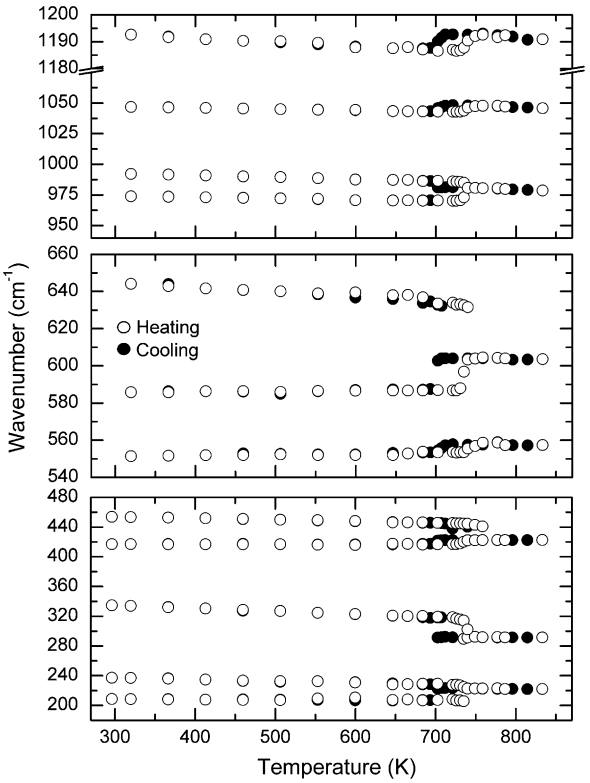

Fig. 2. The Raman mode frequencies of $BaZr(PO_4)_2$ as a function of temperature during heating and cooling across the phase transition temperature near 730 K.

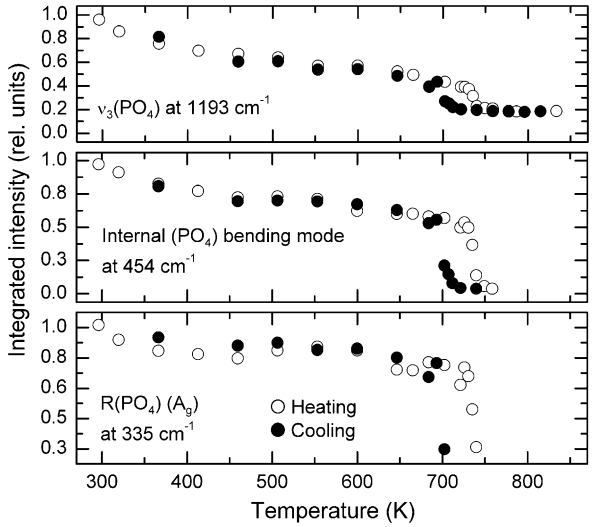

Fig. 3. The Raman band intensities of $BaZr(PO_4)_2$ as a function of temperature during heating and cooling across the phase transition temperature near 730 K.

The onset of a sharp decrease in the intensity near 730 K as seen in Fig. 3 nicely coincides with an endothermic effect at 733 K which has previously been detected by differential thermal analyses [5,6]. However, some bands (e.g., the band near 454 cm^{-1}) can be traced up to a temperature of 755 K, indicating a two-phonon-like behavior. This demonstrates that clusters larger than about 10 Å of both polymorphs still coexist above the transition temperature. On cooling, some bands already appear near 730 K (Figs. 1 and 2), but a dramatic intensity increase occurs between 710 and 700 K. This interval also matches well with the exothermic effect observed by DTA at 710 [5] and 705 K [6], respectively. We further note that the frequencies of the antisymmetric $\nu_3(PO_4)$ stretching bands at 1047 and 1193 cm^{-1} shift to higher frequencies at the transition temperature on heating (Fig. 2), indicating a slight shorting of the P–O bonds, i.e. a decrease of the volume of the PO_4 tetrahedron.

5. Discussion

5.1. The structure of the high-temperature polymorph

The most significant observation in the present work is the reduction of the overall number of bands during transition considering that, based on X-ray diffraction data, the most likely crystal structure of the high-temperature polymorph is either orthorhombic or hexagonal (trigonal) [5,6], since predicted Raman spectra from trigonal and hexagonal systems are usually much simpler than those from orthorhombic crystals. To test both possibilities, we considered, at first, only the reduction of the number of internal PO_4 modes and carried out site-to-factor group correlation analyses [8] for possible site symmetries of the $(PO_4)^{3-}$ anions in all orthorhombic factor groups. The correlation method takes account of (1) the possible effect of the site symmetry and (2) the possible vibrational coupling between different equivalent molecules in the unit cell on the selection rules. In this respect, we note here that the site group must be a subgroup of both the molecular point group of the free $(PO_4)^{3-}$ ion, which is $T_d(\bar{4}3m)$, and the factor group. Possible factor groups or point groups, which are isomorphic with the factor groups, in the orthorhombic system are $D_2(222)$, $C_{2v}(mm2)$, and $D_{2h}(mmm)$. The possible site groups for the three factor groups, as given by supergroup–subgroup relationships [9], are thus (1) D_2, C_2, and C_1 in D_2, (2) C_{2v}, C_2, C_s, and C_1 in C_{2v}, and (3) D_{2h}, C_{2v}, C_{2h}, C_2, C_s, C_i, and C_1 in D_{2h}. We further note that it was necessary to only consider those sets of sites having a multiplicity of two in the Bravais cell, because the number of $(PO_4)^{3-}$ groups in the Bravais cell has to be small to account for the low number of observed internal PO_4 modes. Note that the vibrational degree of freedom is given by $N(3n–6)$, where N is the number of formula units per unit cell and n is the number of atoms in the $(PO_4)^{3-}$ anion. With two $(PO_4)^{3-}$ groups (and thus one formula unit) in the Bravais cell, one expects 18 vibrational modes. For instance, the C_2 site in the D_{2h} factor group contains more than two equivalent atoms in all orthorhombic space groups and, thus, was not considered. This further reduced the number of possible site groups. The results of the group theoretical survey are summarized in Table 1. It is evident from this table that group theory predicts more vibrational modes in all orthorhombic point

Table 1
Theoretical number of Raman active internal PO_4 modes in the high-temperature polymorph of $BaZr(PO_4)_2$ calculated for two $(PO_4)^{3-}$ groups in the Bravais cell by means of the correlation method [8]

Factor group	Site group	$\nu_1(PO_4)$	$\nu_2(PO_4)$	$\nu_3(PO_4)$	$\nu_4(PO_4)$
Observed		1	1	2	2
$T_d \equiv 4\bar{3}m$ (free PO_4 mol.)		1	1	1	1
$D_2 \equiv 222$ (No. 16–24)	$D_2 \equiv 222$	2	4	6	6
	$C_2 \equiv 2$	2	4	6	6
$C_{2v} \equiv mm2$ (No. 25–46)	$C_{2v} \equiv mm2$	2	4	6	6
	$C_2 \equiv 2$	2	4	6	6
	$C_s \equiv m$	2	4	6	6
$D_{2h} \equiv mmm$ (No. 47–74)	$D_{2h} \equiv mmm$	2	2	3	3
	$C_{2h} \equiv 2/m$	1	2	3	3
	$C_{2v} \equiv mm2$	2	2	4	4
	$D_2 \equiv 222$	1	2	3	3
$S_6 \equiv \bar{3}$ (No. 147–148)	$C_3 \equiv 3$	1	2	3	3
$D_3 \equiv 32$ (No. 149–155)	$C_3 \equiv 3$	1	2	3	3
$C_{3v} \equiv 3m$ (No. 156–161)	$C_3 \equiv 3$	1	2	3	3
$D_{3d} \equiv \bar{3}m$ (No. 162–167)	$C_{3v} \equiv 3m$	1	1	2	2
$C_6 \equiv 6$ (No. 168–173)	$C_3 \equiv 3$	2	2	3	3
$C_{3h} \equiv \bar{6}$ (No. 174)[a]	$C_3 \equiv 3$	1	2	3	3
$C_{6v} \equiv 6mm$ (No. 183–186)	$C_{3v} \equiv 3m$	1	2	3	3
$D_{3h} \equiv \bar{6}m2$ (No. 187–190)	$C_{3v} \equiv 3m$	1	2	3	3
$D_{6h} \equiv 6/mmm$ (No. 191–194)	$C_{3v} \equiv 3m$	1	2	3	3

[a]Note that the hexagonal space groups 175–182 do not contain site symmetries, which have a multiplicity of two in the Bravais cell and are also subgroups of both the molecular point group of a free $(PO_4)^{3-}$ molecule and the factor group.

groups than experimentally observed, which precludes an orthorhombic cell for the high-temperature polymorph. Next, we repeated the same procedure for all trigonal and hexagonal space groups and found that mode splitting in the site group C_{3v} along with the vibrational coupling of the two $(PO_4)^{3-}$ groups in a unit cell of D_{3d} symmetry is the only combination that accounts for the observed reduction of the number of internal PO_4 bands (Table 1). This finding leaves $D^1_{3d}(P\bar{3}1m)$, $D^3_{3d}(P\bar{3}m1)$, and $D^5_{3d}(R\bar{3}m)$ as possible space groups for the high-temperature polymorph of $BaZr(PO_4)_2$. The correlation between the molecular, site, and factor group for the PO_4 vibrations is given in Table 2 along with the correlation between the factor groups of the low- and high-temperature polymorph.

We then evaluated the site symmetries of Zr, Ba, and O. Due to the fact that there are two different D_{3d} sites with a multiplicity of one in all three possible space groups and that the translational movements of both cations are apparently not Raman active (note that we have not detected new low-frequency modes in the Raman spectrum), the Ba and Zr atoms must occupy a D_{3d} site. Furthermore, one O atom, O(1), of the PO_4 tetrahedron must lie on a three-fold axis as well as on a mirror plane (with C_{3v} symmetry) and the other three O atoms, O(2), must lie on a mirror plane to account for the C_{3v} symmetry of the PO_4 tetrahedron. The O(1) atom is thus located at the top vertices and the O(2) atoms form the base of the tetrahedron. The two PO_4 tetrahedra are thus characterized by two different bond lengths P–O(1) and P–O(2). In the diatomic approximation, which assumes that each polyhedron is separated from the crystal lattice and that each distinct bond is vibrationally independent of the lattice, each single bond is assumed to exhibit a unique stretching frequency reflecting its bond length. Popović and coworkers [10] have recently shown that the stretching frequencies of the PO_4 tetrahedron in phosphates correlate linearly with the assigned P–O bond lengths determined by X-ray diffraction. By using their empirical correlation and assigning the highest and lowest observed stretching frequency of the high-temperature at 835 K polymorph to the shortest and longest bond, respectively, we obtain P–O bond lengths of 0.149 and 0.155 nm.

Finally, we carried out the group theoretical analysis with these site symmetries in the D_{3d} factor group and obtained the irreducible representations summarized in Table 3. Subtraction of the two acoustic modes ($\Gamma_{acoustic} = A_{2u} + E_u$) yielded 13 IR active and nine Raman active modes. From the nine predicted Raman active modes, we have observed eight in the frequency range between 160 and 1300 cm^{-1} (Fig. 1). Based on the group theoretical prediction, one further external Raman band is thus expected to occur at a frequency below 160 cm^{-1}.

It is interesting to compare the Raman spectrum of the high-temperature polymorph with $A_3(PO_4)_2$ compounds where A = Ba and Sr, which crystallize in the $D^5_{3d}(R\bar{3}m)$ space group [11]. Furthermore, the paraelastic β-phase of $Pb_3(PO_4)_2$, which forms during a ferroelastic phase transition at 453 K from the monoclinic ferroelastic α-phase, has a D^5_{3d} structure [12]. The PO_4 tetrahedra in these trigonal compounds are located on C_{3v} sites and,

Table 2
Correlation table for the internal PO_4 vibrations in the low- and high-temperature polymorph of $BaZr(PO_4)_2$ and the symmetry correlation between both polymorphs

	$(PO_4)^{3-}$ ion	Low-temperature polymorph at 295 K		High-temperature polymorph at 835 K		
	T_d	Site group C_s	Factor group C_{2h}	Transition	Factor group D_{3d}	Site group C_{3v}
$\nu_1(PO_4)$	A_1	A′	A_g, B_u		A_{1g}, A_{2u}	A_1
$\nu_2(PO_4)$	E	A′, A″	A_g, B_u, B_g, A_u		E_g, E_u	E
$\nu_3(PO_4) + \nu_4(PO_4)$	F_2	A′, A′, A″	A_g, B_u, A_g, B_u, B_g, A_u		A_{1g}, A_{2u}, E_g, E_u	A_1, E

Table 3
Atomic positions of the high-temperature polymorph of $BaZr(PO_4)_2$ and predicted mode symmetries

Atom	Multiplicity	Site symmetry	Irreducible representation[a]
Ba	1	$D_{3d}-\bar{3}m$	$\Gamma_{Ba}=A_{2u}(IR)+E_u(IR)$
Zr	1	$D_{3d}-\bar{3}m$	$\Gamma_{Zr}=A_{2u}(IR)+E_u(IR)$
P	2	$C_{3v}-3m$	$\Gamma_P=A_{1g}(R)+E_g(R)+A_{2u}(IR)+E_u(IR)$
O(1)	2	$C_{3v}-3m$	$\Gamma_{O1}=A_{1g}(R)+E_g(R)+A_{2u}(IR)+E_u(IR)$
O(2)	6	C_s-mC_s-m	$\Gamma_{O2}=2A_{1g}(R)+A_{2g}(0)+3E_g(R)+A_{1u}(0)+2A_{2u}(IR)+3E_u(IR)$

[a](IR) Infrared active; (R) Raman active; (0) silent mode.

Table 4
Proposed symmetry assignment of Raman bands (observed at 835 K) of the high-temperature polymorph of $BaZr(PO_4)_2$

	Frequency of the free $(PO_4)^{3-}$ ion (cm^{-1})[a]	Observed frequencies (cm^{-1})[b]	Mode assignment	Type of vibration[c]
$\nu_3(PO_4)$	1017	1191 (w)	A_{1g}	o-o-p P–O(1) stretching
		1046 (s)	E_g	i-p P–O(2) stretching
$\nu_1(PO_4)$	938	979 (vs)	A_{1g}	symmetric P–O stretching
$\nu_4(PO_4)$	567	604 (w)	A_{1g}	o-o-p O(2)–P–O(1) bending
		557 (vw)	E_g	i-p O(2)–P–O(2) bending
$\nu_2(PO_4)$	420	423 (s)	E_g	symmetric O–P–O bending

[a]Frequencies were taken from [15].
[b]vw: very weak; w: weak; s: strong; vs: very strong intensity.
[c]o-o-p: out of plane; i-p: in-plane.

accordingly, their Raman spectra also exhibit six internal PO_4 bands [12–14].

5.2. Assignment of the internal PO_4 bands of the high-temperature polymorph

The strongest Raman active internal PO_4 band at 979 cm^{-1} (835 K) can clearly be assigned to the symmetric (A_{1g}) $\nu_1(PO_4)$ stretching motions of all four oxygen atoms in the PO_4 tetrahedron because the $\nu_1(PO_4)$ vibration in orthophosphates has a lower frequency than the $\nu_3(PO_4)$ stretching modes [10], which have A_{1g} and E_g symmetry. The movement of the O atoms during the E_g stretching vibration occurs within the basal plane of the tetrahedron, whereas during the A_{1g} stretching vibration the O atoms vibrate out of this plane. It is not obvious which of the observed two stretching bands can be assigned to the two symmetries. However, Benoit and Chapelle [12] have shown by polarized Raman measurements that for the trigonal β-phase of $Pb_3(PO_4)_2$ the highest frequency mode has A_{1g} symmetry. Since there is a clear separation between internal and external modes in $BaZr(PO_4)_2$ as in $Pb_3(PO_4)_2$, it is unlikely that the difference of the cation sublattice could dramatically alter the internal P–O bonding forces and we thus assign the A_{1g} and E_g symmetry to the bands at 1191 and 1046 cm^{-1}, respectively. If this is correct, the PO_4 tetrahedron is slightly compressed in the direction of the three-fold rotation axis (see Section 5.1).

The assignment of the three internal bending modes is also not straightforward. However, if we assume that in $BaZr(PO_4)_2$ the symmetrical $\nu_2(PO_4)$ bending mode with E_g symmetry has a lower frequency than the two $\nu_4(PO_4)$ antisymmetric bending vibrations, the bands at 604 and 557 cm^{-1} at 835 K can be assigned to a $\nu_4(PO_4)$ bending mode. This assumption follows from a general wavenumber order of $\nu_3>\nu_1>\nu_4>\nu_2$, which is often valid for molecular crystals where kinematic mode coupling is limited or does not occur as in free molecules (see Table 4). Note also that such assignment is in agreement with the observation that symmetrical bending vibrations of a relative isolated tetrahedron result in a stronger polarizability, i.e., a higher Raman intensity, than antisymmetric bending vibrations (see Fig. 1a). The assignment of both ν_4 modes can again be made by comparison with the assignment of the internal modes in the trigonal β-phase of $Pb_3(PO_4)_2$ [12] and, hence, the bands at 604 and 557 cm^{-1} can be assigned to vibrations of A_{1g} and E_g symmetry, respectively. Accordingly, the remaining internal band at 423 cm^{-1} must be the $\nu_2(PO_4)$ bending mode with E_g symmetry. The proposed symmetry assignment of the observed internal PO_4 bands is summarized in Table 4.

Acknowledgments

K.P. acknowledges the European Commission for support given in the framework of the "Training and Mobility of Researchers" program. H.-W. Meyer is thanked for his comments on an early draft of the manuscript. We further would like to thank two anonymous reviewers for their helpful comments.

References

[1] R.C. Ewing, W.J. Weber, F.W. Clinard Jr., Progr. Nucl. Energy 29 (1995) 63–127.
[2] W.J. Weber, R.C. Ewing, C.R.A. Catlow, T. Diaz de la Rubia, L.W. Hobbs, C. Kinoshita, H. Matzke, A.T. Motta, M. Nastasi, E.K.H. Salje, E.R. Vance, S.J. Zinkle, J. Mater. Res. 13 (1998) 1434–1484.
[3] K. Fukuda, K. Fukutani, Powder Diff. 18 (2003) 296–300.
[4] K. Fukuda, A. Moriyama, S. Hashimoto, J. Solid State Chem. 177 (2004) 3514–3521.
[5] K. Fukuda, A. Moriyama, T. Iwata, J. Solid State Chem. 178 (2005) 2144–2151.
[6] K. Popa, R.J.M. Konings, P. Boulet, D. Bouëxière, Thermochem. Acta 436 (2005) 51–55.
[7] M.Th. Paques-Ledent, J. Inorg. Nucl. Chem. 39 (1977) 11–17.
[8] W.G. Fateley, N.T. McDevitt, F.F. Bentley, Appl. Spectrosc. 25 (1971) 155–173.
[9] G.F. Koster, T.O. Dimmock, R.G. Wheeler, H. Satz, Properties of the Thirty-two Point Groups, MIT Press, Cambridge, 1963.
[10] L. Popović, D. de Waal, J.C.A. Boeyens, J. Raman Spectrosc. 36 (2005) 2–11.
[11] W.H. Zachariasen, Acta Crystallogr. A 1 (1948) 263–265.
[12] J.P. Benoit, J.P. Chapelle, Solid State Commun. 15 (1974) 531–533.
[13] P. Tarte, J. Thelen, Spectr. Chem. Acta 28A (1972) 5–14.
[14] L. Popović, B. Manoun, D. de Waal, J. Alloys Compd. 343 (2002) 82–89.
[15] A. Mueller, B. Krebs, J. Mol. Spectrosc. 24 (1967) 180–198.